**Manuscript of**

**Electrochimica Acta 94,314-319(2013)**

# *Photoelectrocatalytic performance of $WO_3/BiVO_4$ toward the dye degradation*

Ponchio Chatchai *[1], Atsuko Y. Nosaka[2], and Yoshio Nosaka[2]

[1]Department of Chemistry, Faculty of Science and Technology, Rajamangala University of Technology Thanyaburi, Phathumtani, 12110 Thailand

[2]Department of Materials Science and Technology, Nagaoka University of Technology, Nagaoka, 940-2188 Japan

Received Month XX, 200X; Accepted Month XX, 200X

e-mail: chatchai@rmut.ac.th

Tel: +66-2-5493540

**Abstract**

The photocatalytic (PC) and photoelectrocatalytic (PEC) properties of $WO_3/BiVO_4$ photo-anode for organic dye degradation under visible light irradiation were studied. The performance of the electrodes was investigated by monitoring the % degradation of methylene blue (MB) as a dye sample with UV-Vis spectroscopy. To study the charge transfer rate improvement, a $Cu_2O$ electrode was employed as a photo-cathode. In addition, Ag nanoparticles were deposited on both $WO_3/BiVO_4$ and $Cu_2O$ electrodes to study the effect on the catalytic activity for MB degradation. SEM, XRD and XPS techniques were used to confirm the morphologies and composition of the modified electrodes. The effects of pH and the irradiation wavelengths were investigated to understand the condition of MB degradation process. The highest performance for MB degradation was attained when $WO_3/BiVO_4$ was used as a photo-anode and $Cu_2O$/Ag as a photo-cathode under the PEC process.

*Keyword: Photoelectrocatalysis, $WO_3/BiVO_4$, Methylene blue degradation*

## 1. Introduction

Some organic dyes eluted from textile industries can be significantly dangerous water pollutants. The toxicity and carcinogenic nature of those dyes cause a number of risks to human health. However, the elimination by conventional physical techniques is quite difficult. The photocatalytic degradation techniques of organic dyes would be attractive for the elimination due to its strong oxidation ability, low-cost and environmentally friendly characteristics. The powder suspension of photocatalysts has been studied widely to evaluate the activity. However, powder photocatalysts essentially have a problem because they must be separated from the system after the completion of the catalytic process and the probability of deactivation by electron-hole recombination is high. On the other hand, the photoelectrochemical technique, in which photocatalysts are deposited on transparent electrodes, would make the treatment in practical application much easier and have a potential to enhance charge separation by applying potential to serve higher degradation performance. $TiO_2$ is a widely investigated photocatalyst, but it only responds to the light in ultraviolet region [1-4]. For utilizing solar light, materials of the narrow band gap energy semiconductors which absorb visible light are attractive [5-7]. Although CdS has been used as photocatalysts, it decomposes by oxidation reaction as toxicity of Cd ions became a serious problem. In place of CdS, at present $BiVO_4$ is widely used as yellow pigment. Monoclinic $BiVO_4$ is an excellent semiconductor photocatalysts, which presents a high activity for the oxidization of water and degradation of organic pollutants under visible light irradiation [8-10]. However, pure $BiVO_4$ presents low activity due to the high electron-hole recombination ratio. In order to enhance charge separation in $BiVO_4$ photocatalyst, it must be combined with a semiconductor having a suitable band gap energy level.

In the previous work, we reported that the composite of $SnO_2/BiVO_4$ and $WO_3/BiVO_4$ as photo anodes presented higher photocatalytic activity compared to a pure $BiVO_4$ for water oxidation under visible light irradiation [11, 12]. The combination of $WO_3/BiVO_4$ shows higher activity than $SnO_2/BiVO_4$ because $WO_3$ has more suitable band energy level to separate charge from $BiVO_4$. Moreover, $WO_3$ has been studied extensively to reduce the recombination effect on $TiO_2$ [13-14]. The photocatalytic activities of composite $WO_3/BiVO_4$ were further improved by the modification with Au nanoparticles, which increased charge transfer process without undergoing a plasmon resonance effect [15]. Moreover, we have studied the effect of Pt nanoparticles deposited on $Cu_2O$ as a photo cathode for water reduction under visible light irradiation [16]. The small Pt particle plays a catalyst-function to improve the charge transfer process and the surface roughness of the $Cu_2O$ electrode. We have suggested that the combination of the modified $WO_3/BiVO_4$ as a photo-anode with the modified $Cu_2O$ as a photo-cathode should present a high efficiency for water splitting under visible light irradiation. Therefore, this modified electrode system would be suitable for the application in dye degradation. However, Au and Pt are highly expensive for practical applications. Alternative candidates would be noble Ag nanoparticles. In addition to the low cost, Ag offers a possibility to improve the photocatalytic activity for organic pollutant degradation [17-21].

In this work, we have studied the dye degradation by using $WO_3/BiVO_4$ as a photo-anode under visible light irradiation. The $Cu_2O$ has also been investigated as a photo-cathode to enhance the charge transfer rate. In addition, the effect of Ag

nanoparticle modification on both photo-anode and photo-cathode electrodes were investigated.

## 2. Experimental

### *2.1 Fabrication of $WO_3/BiVO_4$, $Cu_2O$ electrodes and modification with Ag nanoparticles*

Fabrication methods of $WO_3/BiVO_4$ and $Cu_2O$ electrodes were described previously [12, 16]. The electrodeposition technique was employed to deposit Ag nanoparticles in a 1 mM $AgNO_3$ solution containing 2mM sodium citrate and 0.1M $KNO_3$ at the applied potential of -0.6 V vs Ag/AgCl and the deposition time of 30s, respectively [22].

### *2.2 Photoelectrochemical measurements and characterization*

The morphologies of electrode surface were investigated with a scanning electron microscope (SEM), (Technex Co., Tiny-SEM 1710). X-ray photoelectron spectroscopy (XPS) measurements were carried out using a JPS-9010TR spectrometer (JEOL) with a monochromatic MgKα source. X-ray diffraction (XRD) patterns were recorded with a diffract meter (MAC Science, M03HF22) using Cu Kα radiation.

Photocurrent was measured by a three-electrode system, where a Pt wire and $Cu_2O$/Ag were the auxiliary electrode, an Ag/AgCl was the reference electrode, $WO_3/BiVO_4$ and $WO_3/BiVO_4$ modified with Ag nanoparticles were the working electrode. An aqueous solution of 5.0 $mgL^{-1}$ methylene blue in 0.1 M $Na_2SO_4$ was used as a dye sample solution [1, 3]. A voltammetry analyzer (Princeton Applied Research, Inc., VersaSTAT 3) was used in the modes of cyclic voltammetry and linear scan voltammetry. For photo-irradiation, a 50-W tungsten lamp (Moritex,

MHF-C50LR) was used as the light source and an optical filter (Hoya, L-42) was inserted on the light path between the lamp and the test electrode to measure the photocurrent properties at wavelengths longer than 420 nm. For the methylene blue degradation study, a 500 W Xenon lamp (Ushio Denki, X500) was used as a light source and cut-off UV light region with an optical filter (Hoya, L-42). A voltammetry analyzer (Hokuto Denko, HSV-100) was used for applying the potential at 0.2 V vs Ag/AgCl. The concentration of the methylene blue (MB) was determined from the absorbance observed at $\lambda$= 662 nm using a UV/Vis spectrophotometer (Shimadzu, UV-3150). The percentage of MB degradation was calculated using:

$$\% \text{ degradation} = [(A_0-A_t)/A_0\ ] \times 100$$

Where, $A_0$ = absorbance at t = 0 min, $A_t$ = absorbance at t minutes after the irradiation [23].

## 3. Results and discussion

### *3.1 Characterization of the film photocatalysts*

The morphologies of $WO_3/BiVO_4$ electrode and that deposited with Ag nanoparticles are shown in Figures 1A and 1B, respectively. In addition, the SEM image also shows the change of the surface morphology of $Cu_2O$ when deposited with Ag nanoparticles of the particle size in the range of 50-200 nm (Figures 1C and D). As shown in Figures 1B and 1D, the modified Ag nanoparticles on a $WO_3/BiVO_4$ substrate show higher density than that of the $Cu_2O$ surface. Thus, it was confirmed that with the electrochemical technique Ag nanoparticles could be deposited on both $WO_3/BiVO_4$ and $Cu_2O$ surfaces.

XPS spectrum was used to confirm that the Ag metal was deposited on the substrate of $WO_3/BiVO_4$ and $Cu_2O$ (Figures 2A and B), respectively. The chemical

state of Ag on $Cu_2O$ sample have been directly verified with the Ag (0) state from the reference XPS spectrum of Ag metal 3d [24], while the signal of Ag on $WO_3/BiVO_4$ sample shows a chemical shift towards slightly lower binding energy by 0.2 eV. Moreover, for the identification, the crystalline structures of $WO_3/BiVO_4$ and $Cu_2O$ were studied before and after Ag deposition (Figure 3). The crystalline structures of $BiVO_4$ and $Cu_2O$ were confirmed in a similar way to the previous work [12, 15 and 16]. Although the contribution of Ag to the XRD pattern was very small due to a smaller amount of Ag comparing with other components, these results certainly verify the presence of Ag in the composition of the modified electrode.

*3.2 Photocatalytic and Photoelectrocatalytic degradation of methylene blue*

The absorption spectra of MB with different reaction times of photoelectrocatalytic (PEC) process are shown in Figure 4A. All of the absorption peaks of MB decreased with an increase of the degradation time without forming other new peaks, indicating that MB degraded in full mineralization. In Figure 4B, the decrease of the peak absorbance of MB at 662 nm as a function of the irradiation time is shown with different stages for applied potential (EC), photocatalysis (PC), and photoelectrocatalysis (PEC). The highest degradation of MB was attained when both applied potential (EC) and light irradiation (PC) were introduced, that is, PEC showed the highest efficiency for MB degradation. Moreover, under dark conditions without any bias potential, a constant absorbance was observed, indicating a high stability of MB in a normal condition.

*3.3 Effect of pH*

The MB degradation by the PEC process was studied at various pH (Figure 5). Under applied potential of 0.2 V vs Ag/AgCl and visible light irradiation, MB shows high stability in an acidic condition (pH=3.0). The % degradation increased when pH was adjusted to near neutral (pH 6.5 - 9.0) and under a strong basic condition (pH > 10.0) MB was rapidly degraded. The result indicates that MB easily decomposes under the strong basic condition due to the chemical reaction with $OH^-$. Therefore, on employing MB as a model compound for PEC degradation, the experiment should be performed at neutral pH.

*3.4 Effect of light cut-off*

To understand the mechanism of MB degradation, the effect of wavelength region of light irradiation was investigated. Figure 6 shows the % MB degradation under the light irradiation in different wavelength ranges. The light of wavelength longer than 560 nm was absorbed only by MB (see, Figure 4A), in the region of 400-550 nm, only $BiVO_4$ absorption, in the region longer than 400 nm both $BiVO_4$ and MB absorption, and in the region longer than 325 nm absorptions for all materials were observed. The % MB degradation in the range of $BiVO_4$ absorption is high, while MB absorption did not affect the degradation process. Therefore, it was confirmed that the MB degradation depends on the absorption properties of $BiVO_4$. However, $WO_3$ plays important roles to separate the photoelectron from $BiVO_4$ and induce high photo-holes generated on the $BiVO_4$ surface. There presents highly efficient hetero junction electrodes for dyes decomposition which are correlated with the many researches [13, 14].

*3.5 Effect of Ag nanoparticles modification*

In the above experiments, a Pt-wire was used as a counter electrode and $WO_3/BiVO_4$ as a working electrode. In the following experiments, instead of a Pt-wire, $Cu_2O$ was used as a counter electrode to study the enhancement of electron transfer rate. Especially, the effect of the modification with Ag nanoparticles on both $WO_3/BiVO_4$ and $Cu_2O$ electrodes was investigated. The result shows that Ag nanoparticles present catalytic activity for MB degradation only when deposited on a $Cu_2O$ electrode. Figure 7A shows that the photocurrent for the Ag deposited $Cu_2O$ electrode is increased with the applied potential. The catalytic activity of Ag deposited electrodes was confirmed by the study of MB degradation under photocatalytic (PC) and photoelectrocatalytic (PEC) systems as shown in Figure 7B. Both PC and PEC investigations show that Ag deposition could enhance the % MB degradation than the pure $Cu_2O$ electrode. Since the electron transfer rate for the MB oxidation at $WO_3/BiVO_4$ electrode was not enhanced by Ag deposition, the enhancement observed for $Cu_2O$ electrode would arise from the fact that the energy level of Ag is lower than that of the conduction band of $Cu_2O$ [25]. Therefore, highly efficient electron separation from conduction band of $Cu_2O$ via Ag resulted in a higher electron transfer rate in this system.

The mechanism of MB degradation was studied by monitoring $CO_2$ during PEC process. Figure 8A shows that the increase of $CO_2$ concentration is correlated with the % MB degradation. Thus, it was confirmed that the final product was $CO_2$ as suggested from the fact that the absorption spectra of MB in the degradation process showed no other absorption peaks.

A plausible schematic diagram is presented in Figure 8B by the function of PEC for $WO_3/BiVO_4$ as a photo-anode and $Cu_2O$/Ag as a photo-cathode under visible light irradiation. Under visible light irradiation and bias potential, at a photo-anode a

number of holes ($h^+$) are generated to oxidize MB to $CO_2$. The electrons from the photo anode were derived by bias potential, while at the photo cathode the reduction would take place efficiently by the electron transfer from the $Cu_2O$ conduction band to Ag particles. Therefore, the high efficiency of the degradation of MB was achieved.

## 4. Conclusions

With the electrodeposition technique, Ag nanoparticles could be successfully deposited on both $WO_3/BiVO_4$ and $Cu_2O$ electrodes. $WO_3/BiVO_4$ photo-anode electrode showed a high performance for MB degradation under the photoelectrocatalytic (PEC) process. The $Cu_2O$ photo-cathode modified with Ag nanoparticle presented the enhancement of the catalytic activity for MB degradation under both photocatalytic (PC) and PEC systems. MB degradation was significantly influenced by pH of the solution. To study the PEC process, neutral pH was found to be suitable. A plausible schematic diagram by the function of PEC on employing $WO_3/BiVO_4$ as a photo-anode and $Cu_2O/Ag$ as a photo-cathode under visible light irradiation was proposed. Under visible light irradiation and bias potential, at a photo-anode a significant amount of holes ($h^+$) are generated to oxidize MB to $CO_2$. The electrons from the photo anode were drawn by bias potential, while at the photo cathode the reduction would take place efficiently by the electron transfer from $Cu_2O$ conduction band to Ag particles. This leads to the high efficiency of the degradation of MB.

## Acknowledgements

This work was supported for P.C. by Japan student services organization (JASSO) in program of Follow-up Research Fellowship for Fiscal 2012 and partial financial support from the Research, Development and Engineering (RD&E) Fund

through National Nanotechnology Center (NANOTEC), National Science and Technology Development Agency (NSTDA), Thailand (Project P-12-01160)

**References**

[1] J. Li, L. Zheng, L. Li, Y. Xian, L. Jin, J. Hazard. Mater. 139 (2007) 72.

[2] C. Kim, J. T. Kim, K. S. Kim, S. Jeong, H. Y. Kim, Y. S. Han. Electrochim. Acta. 54 (2009) 5715.

[3] L. Yu, Z. Wang, L. Shi, S. Yuan, Y. Zhao, J. Fang, W. Deng. Appl. Catal. B-Environ. 113 (2012) 318.

[4] M. V. B. Zanoni, J. J. Sene, M. A. Anderson. J. Photoch. Photobio. A. 157 (2003) 55.

[5] J. Luo, M. Hepel. Electrochim. Acta. 46 (2001) 2913.

[6] M. Hepel, J. Luo. Electrochim. Acta. 47(2001) 729.

[7] M. Hepel, S. Hazelton. Electrochim. Acta. 50 (2005) 5278.

[8] A. Kudo. Int. J. Hydrogen Energy 31 (2006) 197.

[9] W. Yin, W. Wang, L. Zhou, S. Sun, L. Zhang. J. Hazard. Mater. 173 (2010) 194.

[10] J. Yu, Y. Zhang, A. Kudo. J. Solid State Chem. 182 (2009) 223.

[11] P. Chatchai, Y. Murakami, S. Kishioka, A. Y. Nosaka, Y. Nosaka. Electrochem. Solid-State Lett. 11 (2008) H160.

[12] P. Chatchai, Y. Murakami, S. Kishioka, A. Y. Nosaka, Y. Nosaka. Electrochim. Acta. 54 (2009) 1147.

[13] I. Shiyanovskaya, M. Hepel. J. Electrochem. Soc., 145 (1998) 3981.

[14] I. Shiyanovskaya, M. Hepel. J. Electrochem. Soc., 146 (1999) 243).

[15] P. Chatchai, S. Kishioka, A. Y. Nosaka, Y. Nosaka. Electrochim. Acta. 55 (2010) 592.

[16] P. Chatchai, A. Y. Nosaka, Y. Nosaka. Electrochemistry. 79 (2011) 821.

[17] X. Zhang, Y. Zhang, X. Quan, S. Chen. J. Hazard. Mater. 167 (2009) 911.

[18] Z. F. Jun, C. M. Liang, O. W. Chun. New Carbon Mater. 25 (2010) 348.

[19] Z. Xiong, J. Ma, W. J. Ng, T. D. Waite, X. S. Zhao. Water Research. 45( 2011) 2095.

[20] S. Kohtani, J. Hiro, N. Yamamoto, A. Kudo, K. Tokumura, R. Nakagaki. Catal. Commun. 6 (2005) 185.

[21] S. Ouyang, N. Kikugawa, Z. Zou, J. Ye. Appl. Catal. A-Gen. 366 (2009) 309.

[22] J. C. Bian, Z. Li, Z. D. Chen, H. Y. He, X. W. Zhang, X. Li, G. R. Han. Appl. Surf. Sci. 258 (2011) 1831.

[23] R. T. Sapkal, S. S. Shinde, T. R. Waghmode, S. P. Govindwar, K. Y. Rajpure, C. H. Bhosale. J. Photochem. Photobiol. B. 110 (2012) 15.

[24] R. K. Sahu, K. Ganguly, T. Mishra, M. Mishra, R. S. Ningthoujam, S. K. Roy, L. C. Pathak. J. Colloid. Interf. Sci. 366 (2012) 8.

[25] P. V. Kamat. Pure Appl. Chem. 74(9) (2002) 1693.

**Figure Captions**

**Figure 1.** SEM images of (A) FTO/$WO_3$/$BiVO_4$ (B) FTO/$WO_3$/$BiVO_4$/Ag (C) FTO/$Cu_2O$ and (D) FTO/$Cu_2O$/Ag electrodes

**Figure 2.** XPS Ag 3d spectra on the substrate (A) $WO_3$/$BiVO_4$, and (B) $Cu_2O$ .

**Figure 3.** XRD patterns of (A) FTO/$WO_3$/$BiVO_4$/Ag and (B) FTO/$Cu_2O$/Ag.

**Figure 4. (A)** Absorption spectra of methylene blue in different time degradation of photoelectrocatalysis using $WO_3$/$BiVO_4$ biased to +0.2 V vs Ag/AgCl under irradiation of visible light ( > 420 nm), **(B)** MB degradation profiles under conditions of (Dark);without light and applied potential, (EC);electrochemical at an applied potential of 0.2V vs Ag/AgCl, (PC);photocatalysis with visible light irradiation (> 420nm), (PEC);photoelectrocatalysis with applied potential of 0.2 V vs Ag/AgCl and visible light irradiation ( > 420nm).

**Figure 5.** The effect of pH on the % degradation of MB by the photoelectrocatalysis with a $WO_3$/$BiVO_4$ electrode, applied potential of 0.2 V vs Ag/AgCl and visible light irradiation ($\lambda$ > 420 nm).

**Figure 6.** The % degradation of MB of $WO_3$/$BiVO_4$ electrode as a function of the irradiation time with the effect of cut-off wavelength of the light. Applied potential was 0.2 V vs Ag/AgCl.

**Figure 7.** (A) Linear scan voltammograms of $WO_3/BiVO_4$ as a working electrode, $Cu_2O$ as a counter electrode in solution of 5.0 mg/L MB and 0.1M $Na_2SO_4$ under dark condition and light irradiation. (B) MB degradation profiles with different stages by using $Cu_2O$ and that modified with Ag nanoparticles as a counter electrode.

**Figure 8.** (A) $CO_2$ production and MB degradation as a function of irradiation time by PEC system of $WO_3/BiVO_4$ as a photo-anode and $Cu_2O$/Ag as a photo-cathode. (B) A schematic diagram of MB degradation under visible light irradiation in this PEC system.

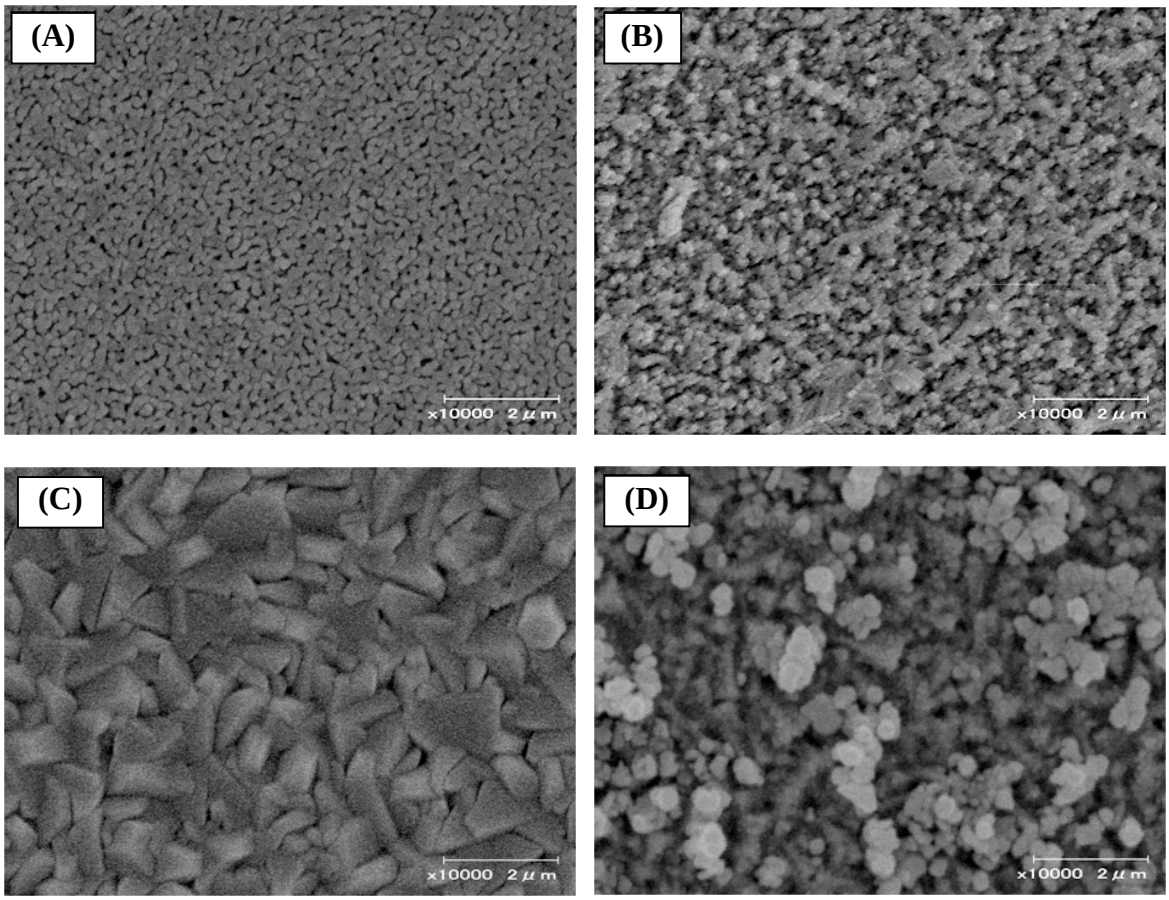


**Figure 1.** SEM images of (A) FTO/$WO_3$/$BiVO_4$ (B) FTO/$WO_3$/$BiVO_4$/Ag (C) FTO/$Cu_2O$ and (D) FTO/$Cu_2O$/Ag electrodes

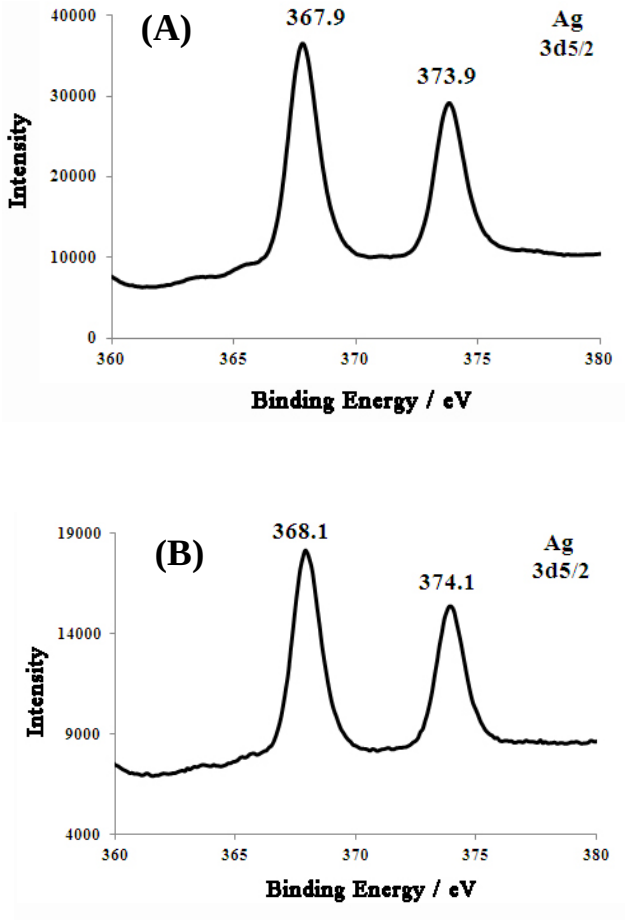


**Figure 2.** XPS Ag 3d spectra on the substrate (A) $WO_3/BiVO_4$, and (B) $Cu_2O$

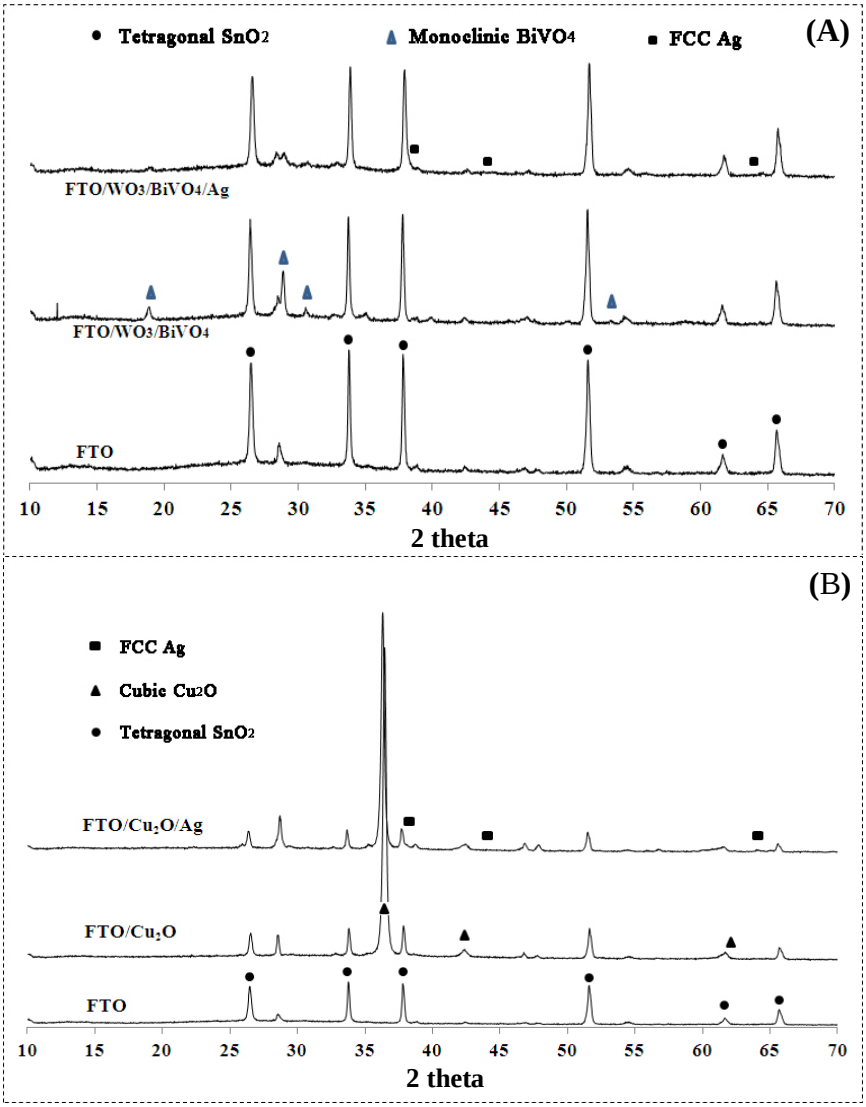


**Figure 3.** XRD patterns of (A) FTO/$WO_3$/$BiVO_4$/Ag and (B) FTO/$Cu_2O$/Ag.

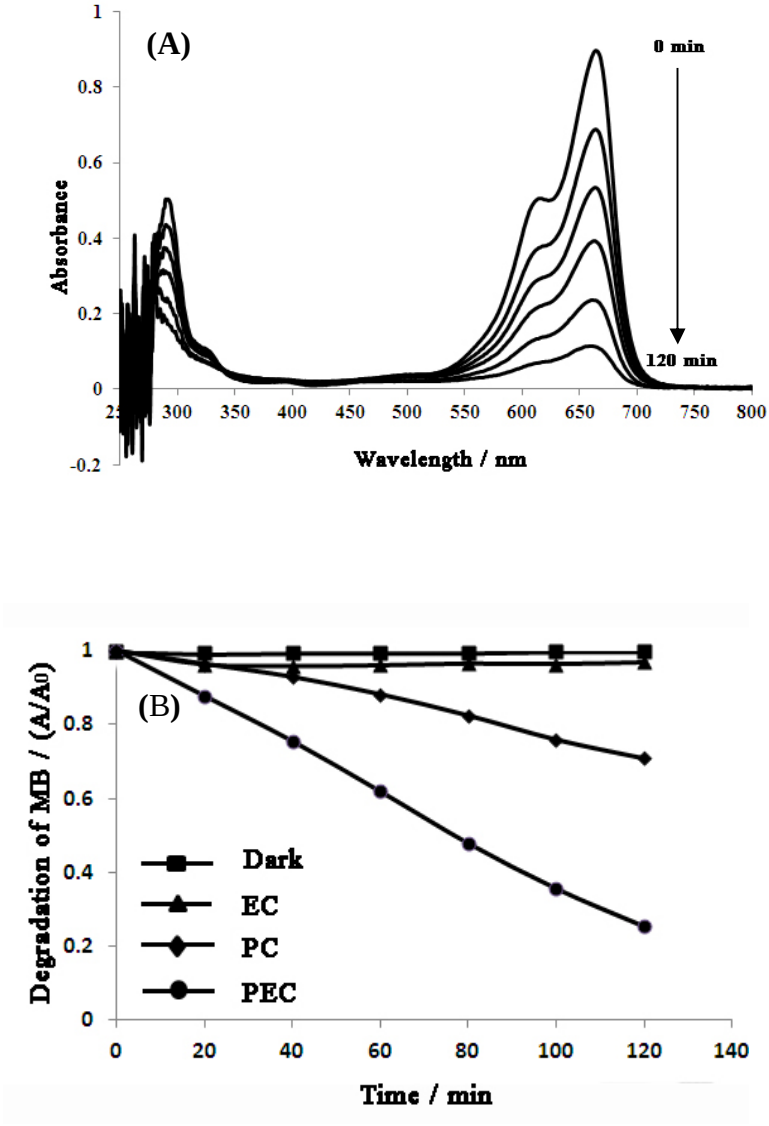


**Figure 4. (A)** Absorption spectra of methylene blue in different time degradation of photoelectrocatalysis using $WO_3/BiVO_4$ biased to +0.2 V vs Ag/AgCl under irradiation of visible light ( > 420 nm), **(B)** MB degradation profiles under conditions of (Dark);without light and applied potential, (EC);electrochemical at an applied potential of 0.2V vs Ag/AgCl, (PC);photocatalysis with visible light irradiation (> 420nm), (PEC); photoelectrocatalysis with applied potential of 0.2 V vs Ag/AgCl and visible light irradiation ( > 420nm).

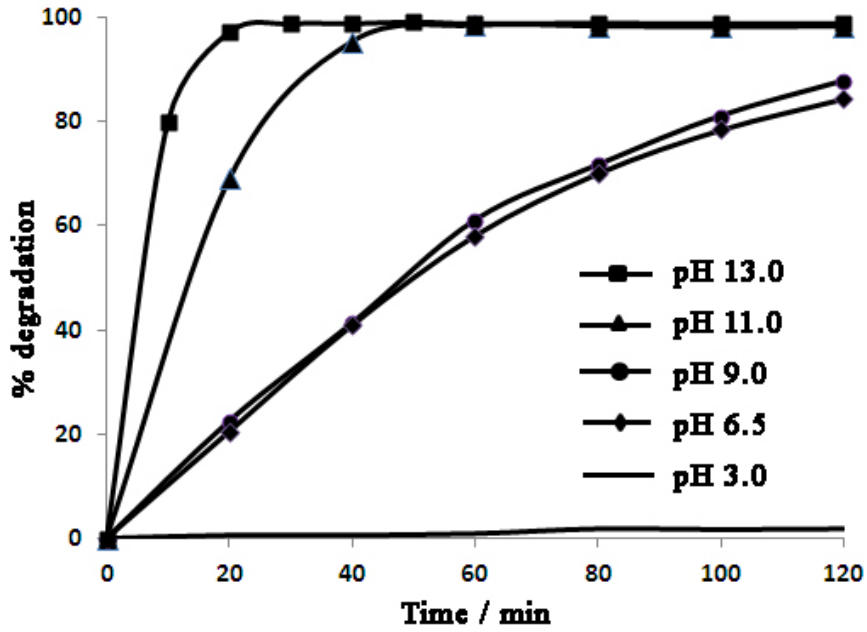


**Figure 5.** The effect of pH on the % degradation of MB by the photoelectrocatalysis with a $WO_3/BiVO_4$ electrode, applied potential of 0.2 V vs Ag/AgCl and visible light irradiation ($\lambda > 420$ nm).

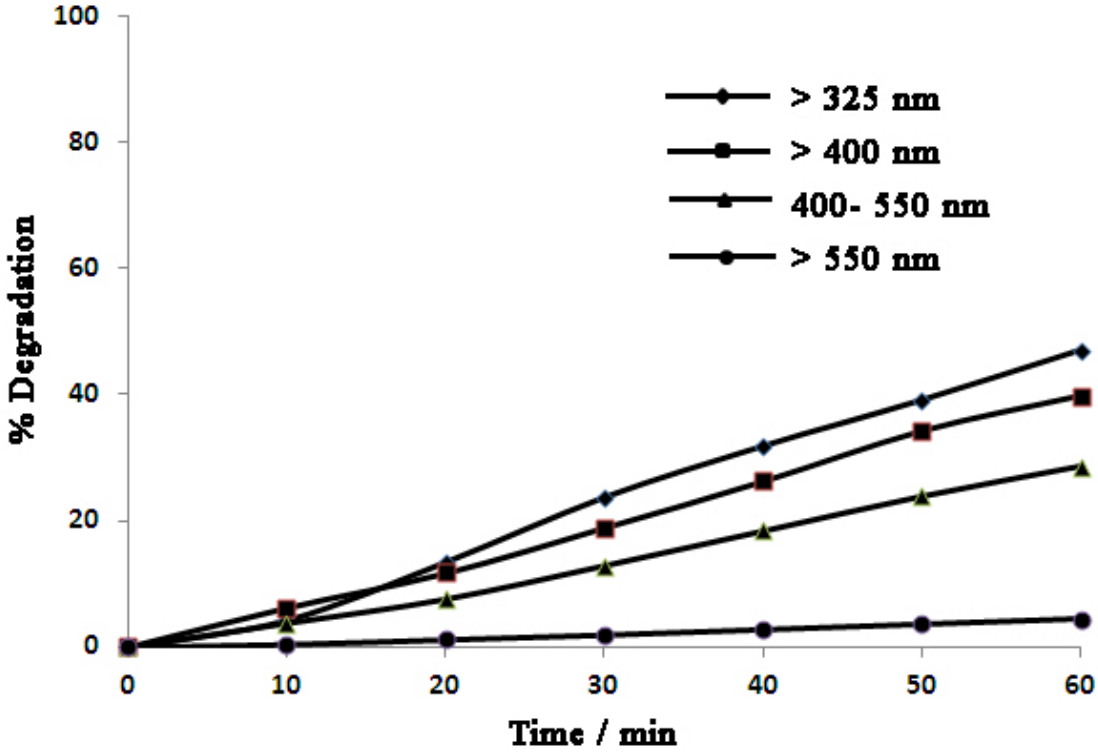


**Figure 6.** The % degradation of MB of $WO_3/BiVO_4$ electrode as a function of the irradiation time with the effect of cut-off wavelength of the light. Applied potential was 0.2 V vs Ag/AgCl.

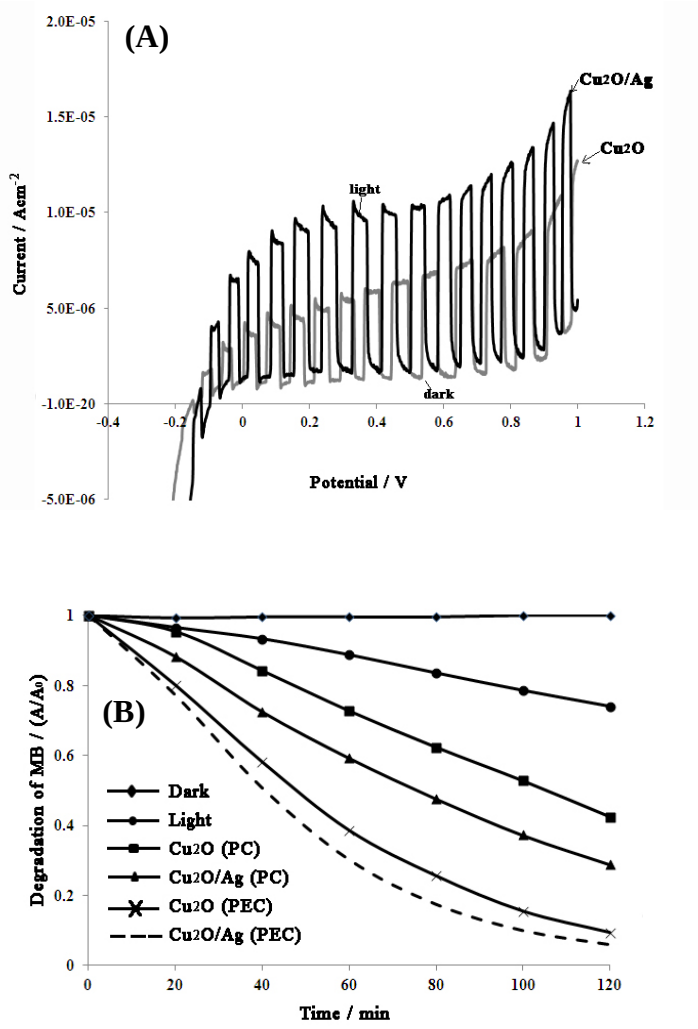


**Figure 7.** (A) Linear scan voltammograms of $WO_3/BiVO_4$ as a working electrode, $Cu_2O$ and $Cu_2O/Ag$ as a counter electrodes in solution of 5.0 mg/L MB and 0.1M $Na_2SO_4$ under dark condition and light irradiation. (B) MB degradation profiles with different stages by using $Cu_2O$ and that modified with Ag nanoparticles as a counter electrode.

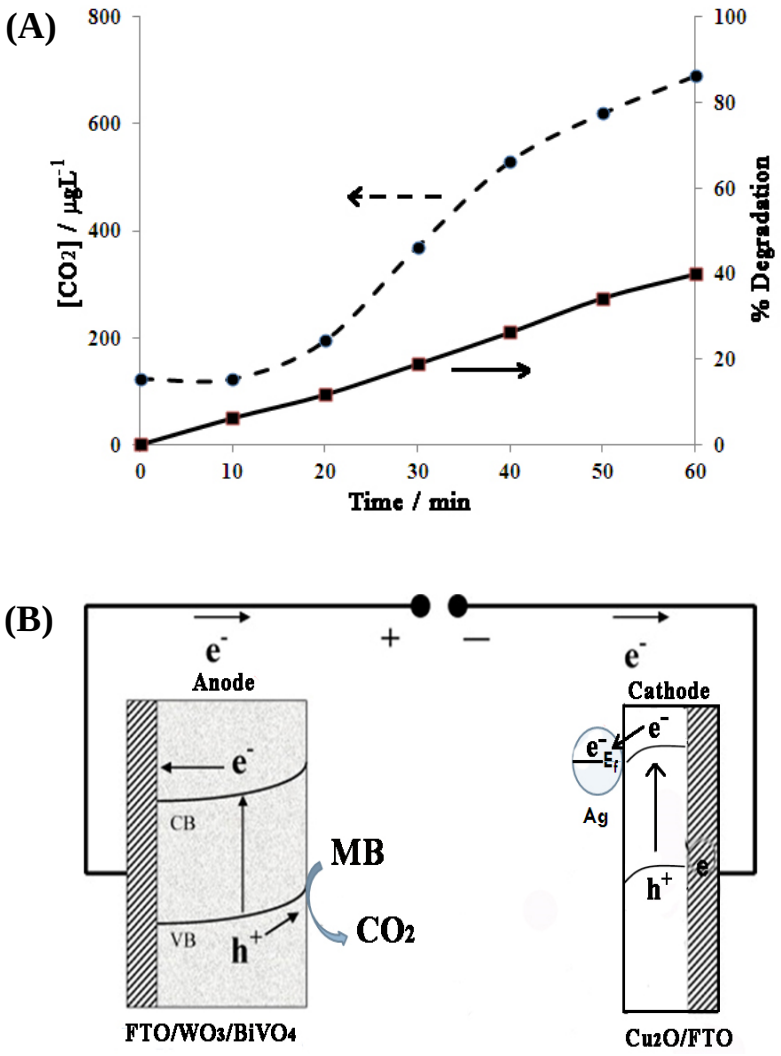


**Figure 8.** (A) $CO_2$ production and MB degradation as a function of irradiation time by PEC system of $WO_3/BiVO_4$ as a photo-anode and $Cu_2O$/Ag as a photo-cathode. (B) A schematic diagram of MB degradation under visible light irradiation in this PEC system